Dual-sensor technique for characterization of carrier lifetime decay transients in semiconductors

R. K. Ahrenkiel,[1,2] S. W. Johnston,[1] D. Kuciauskas,[1] and Jerry Tynan[1]
[1]*National Renewable Energy Laboratory, Golden, Colorado 80401, USA*
[2]*Lakewood Semiconductor LLC, Lakewood, Colorado 80232, USA*

(Received 5 October 2014; accepted 19 November 2014; published online 5 December 2014)

This work addresses the frequent discrepancy between transient photoconductive (PC) decay and transient photoluminescence (PL) decay. With this dual- sensor technique, one measures the transient PC and PL decay simultaneously with the same incident light pulse, removing injection-level uncertainty. Photoconductive decay measures the transient photoconductivity, $\Delta\sigma(t)$. PCD senses carriers released from shallow traps as well as the photo-generated electron-hole pairs. In addition, variations in carrier mobility with injection level (and time) contribute to the decay time. PL decay senses only electron-hole recombination via photon emission. Theory and experiment will show that the time dependence of the two techniques can be quite different at high injection. [http://dx.doi.org/10.1063/1.4903213]

I. INTRODUCTION

Measurement of the minority-carrier lifetime of photovoltaic materials is a critical technique for evaluation of materials and for device manufacture. There are numerous complicating physical effects that appear in the measurement techniques that mask the true excess carrier lifetime. The time-dependent transient techniques contain an abundance of information on the important physical processes that control carrier transport and recombination. Theory shows an intrinsic variation between transient photoconductive decay and transient photoluminescence decay. These effects can be viewed as a source of additional information, rather than a source of conflict between measurements. Photoconductive decay senses the conductivity of all excess carriers—both majority and minority carriers—whereas photoluminescence decay senses only direct electron-hole recombination via photon emission. For example, the radiative recombination process is very dependent on the excess carrier injection-level except in the low-injection case. Because radiative recombination is the dominant mechanism in the tandem cells used for concentrator technology, these high-injection effects are especially important.

In this work, we focus on a means to identify high-injection effects as they affect photoluminescence and photoconductive decay.

II. EXPERIMENTAL DETAILS

Here, we have combined two techniques into a single instrument that provides measurement of photoconductive decay (PCD) and time-resolved photoluminescence (TRPL) simultaneously. A schematic of the experimental setup is shown in Fig. 1. The PCD data are obtained by the transmission-modulated PCD (TMPCD)[1] method. The probe frequency here was 450 MHz but there were no significant differences between frequencies of 400 to 500 MHz. This frequency range provides a penetration depth of several mm in most semiconductor materials. The detector is a low-Q circuit with a response time of several ns based on measurements of short lifetime samples. Two 20 dB amplifiers, were connected in series in the detector circuit, providing a total gain of 40 dB. Simultaneously, the transient photoluminescence decay data (TRPL) are collected by a photodetector and displayed with the PCD data on a dual-channel digitizer. The combined, simultaneous analog data acquisition provides a unique signature that allows analysis of the transient photoluminescence (PL) and PCD kinetics. The technique leads to a unique method of data interpretation. Here, we present data measured on an epitaxial thin film of GaAs and a crystalline wafer of CdTe. Both materials are direct-bandgap semiconductors.

III. TRANSPORT AND RECOMBINATION THEORY

A. Radiative recombination and transient decay

The theories of radiative recombination and TRPL have been described in the literature.[2] In p-type material, the PL intensity after excess carrier generation is given by

$$I_{PL} = B(pn - n_i^2) \approx B(N_A\Delta n + \Delta n^2), \tag{1}$$

where B is the intrinsic recombination coefficient of the specific material, N_A is the doping density, and Δp and Δn are the injected carrier densities.

Here, one can write:

$$p = p_0(r,t) + \Delta p(r,t),$$
$$n = n_0(r,t) + \Delta n(r,t).$$

The carrier concentrations are functions of both positions, r, and time, t.

Using the notation $\rho = \Delta n(r, t)$, $\Delta p(r, t)$ for the injected carrier density, the rate equation for excess carrier decay is

$$\frac{d\rho}{dt} = -B\left(N_A\rho + \rho^2\right). \tag{2}$$

Assuming uniform spatial concentration, the solution to this equation is

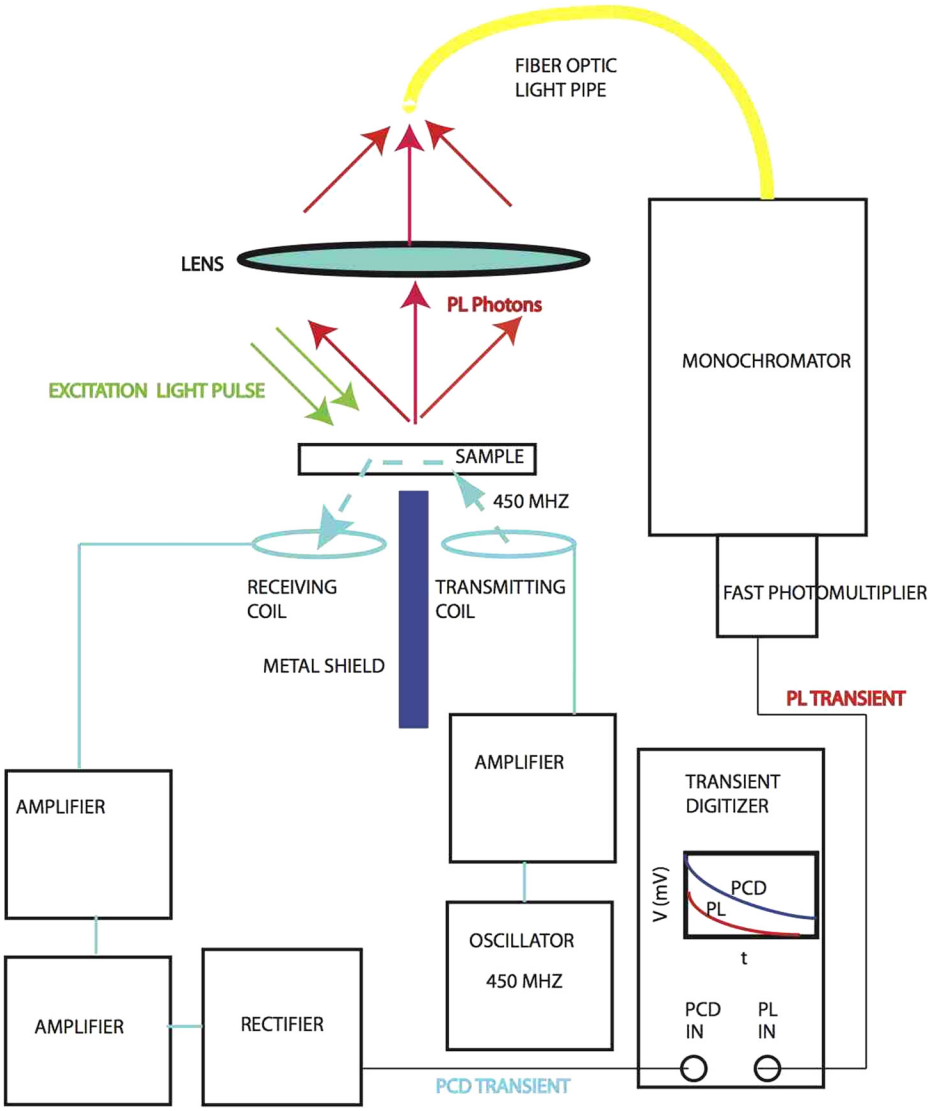

FIG. 1. Dual-sensor apparatus used in the data acquisition system described here.

$$\rho(t) = \frac{\rho_0 \exp(-t/\tau_R)}{1 + \rho_0/N_A(1 - \exp(-t/\tau_R))}. \quad (3)$$

The uniform spatial distribution case is usually approximated in a crystalline thin film such as GaAs. The diffusion process produces a nearly uniform distribution in times much shorter than the carrier lifetime.

In the case of high-quality GaAs epitaxial thin films, radiative recombination dominates and Eq. (3) is applicable.

By substituting Eq. (3) into Eq. (1), the transient PL decay can be calculated. Here, τ_R is the low-injection radiative lifetime defined by

$$\tau_R = \frac{1}{BN_A}. \quad (4)$$

One can see from these equations that the slope of the PL decay, I_{PL}, is steeper than that of the excess carrier density except at low injection. One can show that

$$\tau_{PL} = \frac{N_A + \rho}{N_A + 2\rho}\tau_m. \quad (5)$$

Here, τ_{PL} is the instantaneous PL lifetime and τ_m is the instantaneous recombination lifetime at a given time during the decay process. At very high injection ($\rho > N_A$), the measured PL lifetime is one-half of the actual recombination lifetime, whereas at low injection, they are equal. Thus, at high injection, the instantaneous measured TRPL decay time will be shorter than the PC decay time. The lifetime changes continuously during a transient measurement. However, for steady-state, high-injection conditions (such as in concentrating solar cells), the value appropriate to a given injection level must be applied to the device model. The PL decay time is half of the excess carrier decay time in the limit of very high injection

$$\tau_{PL} = \frac{1}{2}\tau_m. \quad (6)$$

The initial (t = 0) TRPL lifetime at very high injection is

$$\frac{1}{\tau_{PL}} = B(N + 2\rho_0). \quad (7)$$

It is well known that the photoconductive decay, $\Delta\sigma(t)$, varies as $\rho(t)$. The source of the difference between PL and

PC decay data is that the PL decay varies as $\rho(t)^2$ at high injection.

B. Photoconductive decay

The most common measurement of carrier lifetime is based on the measurement of the transient PCD. For the dual-sensor experiments, we used the newly described TMPCD.[1] The transient response following a short pulse of injected excess carriers is given by

$$\Delta\sigma(t) = q\mu_n \Delta n(t) + q\mu_p \Delta p(t). \tag{8}$$

The most common source of excess carrier injection is a short light pulse from a pulsed laser. Recent work on silicon wafers has shown that the mobility changes quite significantly at higher injection levels because of the space-charge effects and the reduced ambipolar mobility. Thus, one should more correctly write the above equation as

$$\Delta\sigma(t) = q\mu_n(\Delta n)\Delta n(t) + q\mu_p(\Delta p)\Delta p(t). \tag{9}$$

C. TRPL simulation and data

One sees from the simulation in Fig. 2 that the PL decay is more rapid than excess carrier decay with an injection level of ten times the dopant level.

1. Ambipolar mobility effects on PCD

The ambipolar mobility change has been well documented in the literature and text books for several decades.[3] The mobility changes were recently measured in thick silicon wafers by combining measurements of transient photoconductive decay with transient free-carrier decay (FCA).[4,5] Because the conductivity, $\sigma(t)$, varies directly with mobility, μ, and the free-carrier absorption coefficient varies as the inverse of mobility, $1/\mu$, the correct mobility could be determined by combining the two data sets.

PCD techniques, including TMPCD, measure the transient conductivity and not the excess carrier density. One can write the PCD signal as

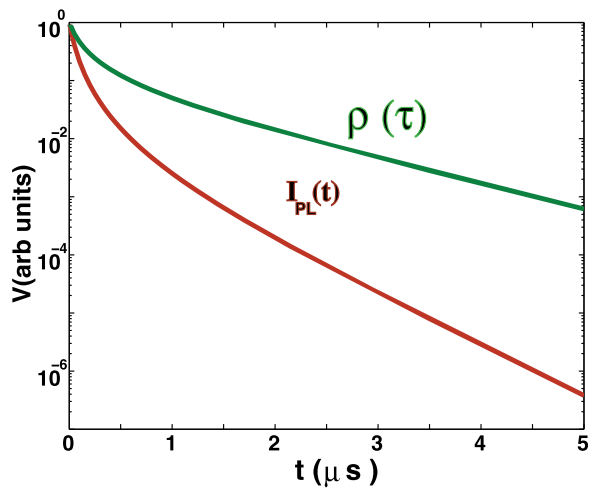

FIG. 2. Simulation of excess carrier decay and PL decay (TRPL) for doping of 1×10^{15} and injection level of $1 \times 10^{16}\text{cm}^{-3}$. Here, the radiative recombination is assumed to be the only effective mechanism.

$$\frac{d\sigma(t)}{dt} = q\mu \frac{d\rho(t)}{dt} + q\rho(t)\frac{d\mu(t)}{dt}. \tag{10}$$

Whereas, $\rho(t)$ decreases after pulse excitation, recent work on silicon wafers has shown that $\mu(t)$ increases after very high injection. The increase is due to space-charge-limited currents (SCLC) and the resultant ambipolar mobility decreased. Therefore, the transient PCD decay may be much longer than the excess carrier density time after a high-injection pulse. The reason for this difference is that the mobility increase compensates the carrier density decrease in this range. Therefore, the PCD is not an accurate metric of carrier lifetime, unless the mobility variation can be accurately calculated or measured.

D. Mobility variation with injection level

The variation of mobility with injection level in silicon was recently demonstrated by Feldman and coworkers[4–6] in silicon wafers, as described above. When the drift-diffusion equations are coupled via the Poisson equation, the resultant ambipolar mobility is given by Ref. 3. In this case, the electron-hole transport is coupled by the internal space-charge and resulting electric fields

$$\mu_{am} = \frac{\mu_p(n,p)\mu_n(n,p)(n-p)}{n\mu_n(n,p) + p\mu_p(n,p)}. \tag{11}$$

This mobility represents the very low field ambipolar mobility in which the internal electric fields are much larger than the external driving fields. The effective mobility is reduced by the requirement of local charge neutrality that opposes electron-hole separation.

The electron and hole mobilities are functions of n and p, where

$$n = N_D + \rho, \quad \text{and} \quad p \approx \rho \tag{12}$$

for n-type material. The transient photoconductivity is

$$\sigma_{pc} = q\rho(t)\mu_{am}(\rho). \tag{13}$$

At very low injection, the photoconductive signal is proportional to the injected carrier density or

$$\sigma_{pc} = q\rho(t)\mu_n(N_D). \tag{14}$$

At very high injection, $\rho \gg \text{N}_\text{D}$, the photoconductivity becomes

$$\sigma_{pc} \approx qN_D \frac{\mu_n(\rho, N_D)\mu_p(\rho)}{\mu_n(\rho, N_D) + \mu_p(\rho)}. \tag{15}$$

The photoconductivity is independent of the injection level except for the decreases in mobility due to carrier-carrier scattering. These effects were recently demonstrated in crystalline silicon wafers.[4–6] In the data of Feldman and coworkers, the initial photoconductive signal increases with time until the injected carrier concentration decreases to

levels such that the mobility begins to increase with time. These effects were seen by combining the transient free-carrier absorption with the transient PCD in separate measurements. The free-carrier absorption varies as ρ/μ, whereas the PCD varies as $\rho * \mu$. By combining the data, the values of $\rho(t)$ and $\mu(t)$ could be uniquely determined.

The free-carrier absorption technique employed by Feldman and coworkers is not applicable to thin films. The free-carrier absorption is very weak and only observable in wafers of thicknesses of several hundred microns in our apparatus. However, these mobility variations are quite measureable in thin films by transient PCD. This is one of the reasons for developing the dual-sensor technique, because any uncertainty about injection level is removed.

IV. EXPERIMENTAL RESULTS

A. GaAs/GaInP double heterostructure

The first sample data presented here were obtained from a GaAs/GaInP double heterostructure (DH) thin film grown by metal-organic chemical vapor deposition. The sample was not intentionally doped, but the background doping is in the $7 \times 10^{15}\,\mathrm{cm}^{-3}$ range and the thickness is $2\,\mu$m. The simultaneous TRPL and TMPCD data from this sample are shown in Figs. 3 and 4, respectively. The lowest-injection data of the GaAs DH are shown in Fig. 5. These data show that the initial decay times vary by about a factor of two. The injection level here is estimated at $3 \times 10^{15}\,\mathrm{cm}^{-3}$. The calculations show weak injection effects according to the decay behavior.

The data associated with the highest injection level are co-plotted in Fig. 6. One sees that the initial time constant for the TRPL data is $0.1\,\mu$s, whereas that of the corresponding TMPCD data are $1.62\,\mu$s. Applying the known B-coefficient of GaAs[6] to Eqs. (2) and (3), one calculates that the initial injection level is $3.3 \times 10^{17}\,\mathrm{cm}^{-3}$. The light pulse was attenuated by calibrated neutral-density filters, allowing measurement with lower injection levels. Therefore, the very high injection level will produce an initial ambipolar mobility reduction at $(t = 0)$ and the mobility will increase as the carrier density, $\rho(t)$, decreases. The latter partially offsets the decrease in excess-carrier concentration produced by recombination. The net effect is to produce a transient photoconductive signal that has a decay time transient that is much larger than the actual recombination lifetime.

We see that the data have very similar characteristics to the plots in the simulation studies shown in Figs. 7 and 3. The relatively slow response of the PCD is related to the mobility reduction at very high injection levels. The very steep decay of the PL decay at high injection is attributed to

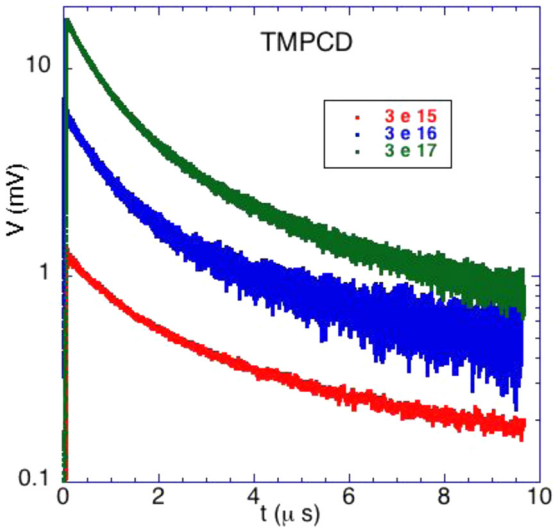

FIG. 4. TMPCD data taken simultaneously with the TRPL data of Fig. 2 using the dual-sensor technique. The data associated with each simultaneous measurement are color coded in the figures.

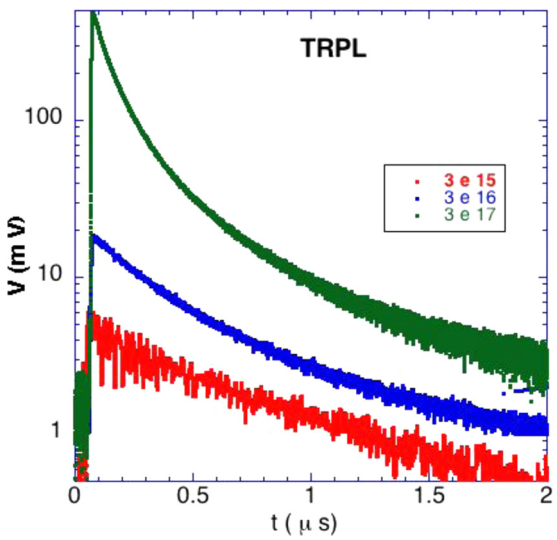

FIG. 3. Time-resolved analog photoluminescence data measured on the GaAs DH sample described in the text. Injection level increased from 3e15 (red) to 3e17 (green). The nonexponential (bimolecular) behavior at high injection is evident in the figure.

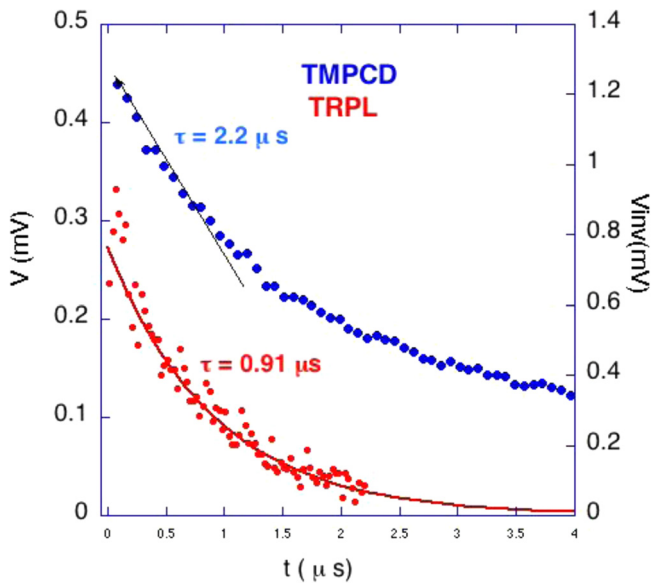

FIG. 5. The lowest injection level measurement of the GaAs DH that was used in these studies. The initial injection level is $3 \times 10^{15}\,\mathrm{cm}^{-3}$.

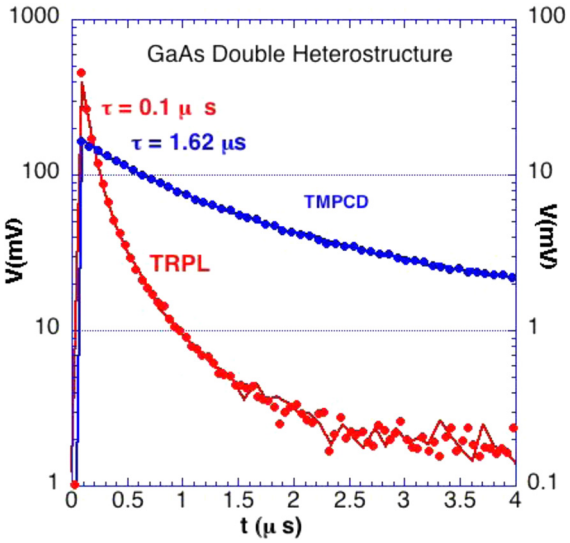

FIG. 6. Co-plot of TMPCD and TRPL data for the GaAs DH with an initial injection level of about $3 \times 10^{17}\,cm^{-3}$.

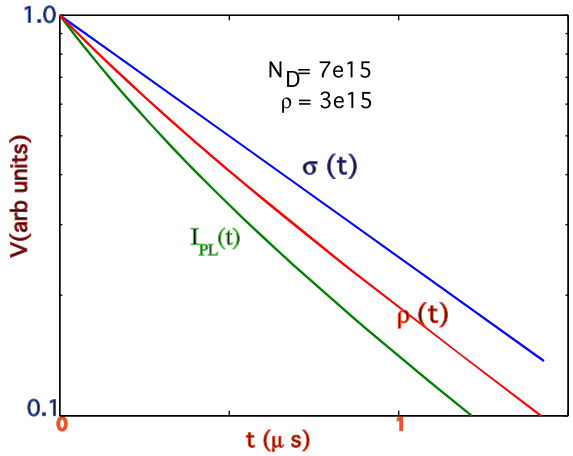

FIG. 7. Simulation of low-injection measurement of GaAs by TRPL and PCD, which includes the ambipolar mobility change with injection level. Here, the assumption is that carrier diffusion has distributed the optically injected carriers uniformly throughout the sample in times much shorter than the observation time.

the increased radiative recombination rate that is derived in Eqs. (2) and (3). In this range, the instantaneous lifetime varies as $1/\rho^2$. Therefore, we expect quite different transient behaviors for TRPL and simultaneous PCD. The latter would be demonstrated by any of the PCD transient techniques.

B. Crystalline CdTe

A second sample used in these studies is a bulk crystalline wafer of CdTe. This sample is a 0.8-mm-thick, single-crystal CdTe sample from JX Nippon Mining & Metals USA, Inc. This sample is 1 cm × 1 cm in size, is nominally undoped, and has a background hole concentration of about $7 \times 10^{15}\,cm^{-3}$. The sample surface was unpassivated. This sample is the subject of a recent publication[7] that uses simultaneous TRPL, microwave PCD, and free-carrier absorption to measure the transient lifetime. Here, we used TMPCD and TRPL in the dual-sensor setup. A doubled YAG laser operating at 532 nm was used as the excitation source. The YAG operates at a 15-Hz pulse rate and has a pulse width of about 5 ns full width at half maximum (FWHM).

The differences in the two data sets are quite remarkable. The TRPL data were obtained by tuning the collection monochromator to the CdTe band edge at 850 nm. The latter data show a very fast response that is near the system response (pulse width and detector rise time). These data are shown in Fig. 8. In contrast, the TMPCD photoconductive decay has a fairly long exponential response of 194 ns, as shown in Figs. 9 and 10.

Measurements were made on the same wafer using the YAG laser set to 1064 nm with quite different effects. Here, two-photon absorption produced deep absorption in the volume of the wafer. The decay time increased to about 139 ns and is similar to the TMPCD results. The fast decay, using 532-nm excitation, can be explained by near-surface excitation and very fast surface recombination prior to diffusion of the excess carriers into the wafer volume. The very short lifetime at $t = 0$ is produced by a very high surface recombination velocity.[8] This effect is combined with self-absorption of the photons generated deeper in the volume of the wafer.

After the initial diffusion of the surviving electrons through the volume of the wafer, a major portion of the emitted photons ($h\nu > E_g$) are self-absorbed in the material. Only those photons in the sub-bandgap PL spectrum, ($h\nu < E_g$), can escape via PL emission. Photon recycling effects[5] for the absorbed photons have been well documented, but are not observable here. Thus, TRPL has excitation-wavelength limitations for lifetime measurement in bulk materials, and weak absorption of the excitation source is required to observe the bulk recombination.

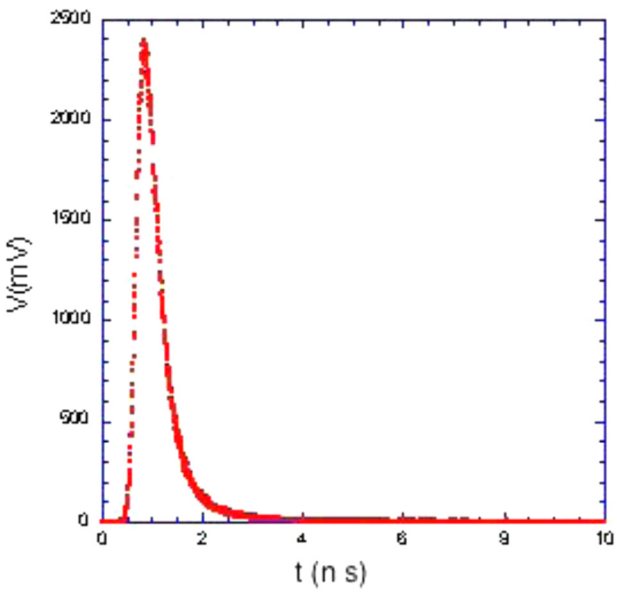

FIG. 8. Analog TRPL data measured on a CdTe single-crystal using the dual-sensor apparatus. The excitation pulse wavelength is 532 nm and the pulse width is 5 ns FWHM.

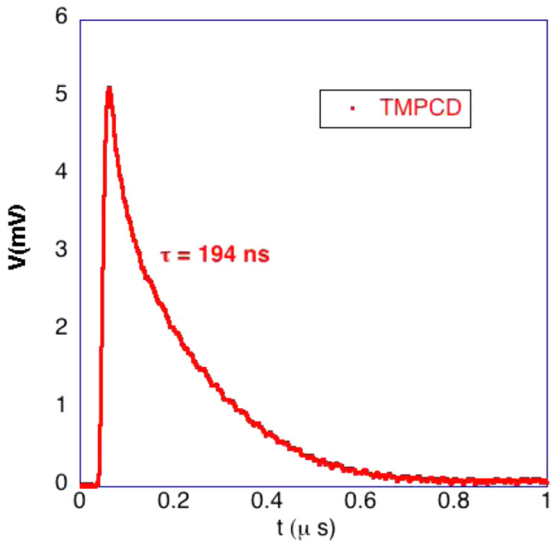

FIG. 9. Simultaneous TMPCD response of the same CdTe wafer using the same 532-nm excitation.

On the other hand, the TMPCD system senses all free carriers that exist throughout the volume because the 500-MHz probe is highly penetrating in the material.

V. SUMMARY

We have shown that several discrepancies exist between the data obtained from time-resolved photoluminescence and transient photoconductive decay. These discrepancies primarily exist at high injection.

(1) The TRPL signal is proportional to the square of the excess carrier density, ρ, at high injection. Therefore, the instantaneous decay rate of the TRPL signal is about half of the actual excess carrier decay rate at any given time in the process.
(2) For thick wafers with an appreciable surface recombination velocity, the real bulk lifetime is masked by the combination of surface recombination and self-absorption of emitted photons in the volume. Thus, the PL decay lifetime may under-represent the real volume lifetime by orders of magnitude.
(3) This issue can be averted by two-photon excitation that provides deep volume excitation. A sufficient number of subbandgap photons escape such that the bulk recombination rate can be measured.
(4) Photoconductive decay also senses the bulk recombination process and provides an appropriate experimental value for the latter.
(5) For thin-film materials, the transient photoconductive decay is greatly lengthened by the low ambipolar mobility that results from space-charge-limited currents at high injection. The TRPL signal is much more representative of the true carrier lifetime.

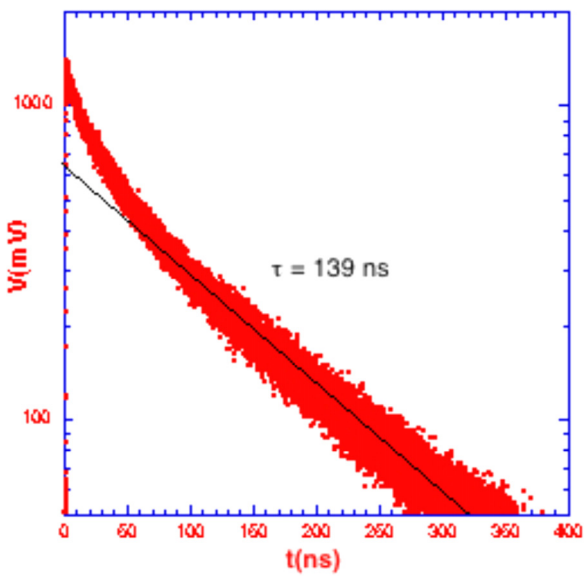

FIG. 10. TRPL on the CdTe single-crystal wafer using two-photon excitation producing deep absorption in the interior of the sample.

VI. CONCLUSIONS

We have shown that there is a different functional dependence between PL(t) and excess-carrier density, ρ(t), at high injection when radiative recombination dominates. At low injection, the functional dependences of signals are quite similar. More significant here is the large mobility reduction that results from space-charge-limited currents at high carrier injection. The SCLC effects produce very large differences between TRPL and PCD as shown by both theory and experiment. These effects can be analyzed and differentiated by the different functional behaviors of the decay transients under these conditions. We found that in thick wafers of direct-bandgap materials, the self-absorption significantly distorts the PL decay curve from the true carrier decay that occurs in the volume of the sample. Two-photon absorption produces more uniform carrier generation throughout the volume of the sample and lessens the latter effect.

None of these single-crystal samples display the long photoconductive "tails" indicative of shallow trapping. The simultaneous measurement of TRPL and PCD is a very effective tool in the measurement and characterization of semiconducting and photovoltaic materials.

ACKNOWLEDGMENTS

This work was supported by the National Renewable Energy Laboratory as a part of the Non-Proprietary Partnering Program under Contract No. DE-AC36-08-GO28308 with the U.S. Department of Energy.

[1]R. K. Ahrenkiel and D. J. Dunlavy, "A new lifetime diagnostic system for photovoltaic materials," Sol. Energy Mater. Sol. Cells **95**, 1985 (2011).
[2]R. K. Ahrenkiel, *Minority-Carrier Lifetime in III-V Semiconductors, Semiconductors and Semimetals* Vol. 39 (Academic Press, New York, 1993), pp. 57–65.
[3]R. A. Smith, *Semiconductors*, 2nd ed. (Cambridge University Press, Cambridge, United Kingdom, 1978).
[4]A. Feldman, R. Ahrenkiel, and J. Lehman, "Transient mobility in silicon as seen by a combination of free-carrier absorption and resonance-coupled photoconductive decay," J. Appl. Phys. **113**, 103703 (2013).
[5]A. Feldman, R. Ahrenkiel, and J. Lehman, "Degradation of photovoltaic devices at high concentration by space charge limited currents," Sol. Energy Mater. Sol. Cells **117**, 408–411 (2013).

[6]R. K. Ahrenkiel, B. M. Keyes, G. B. Lush, M. R. Melloch, M. S. Lundstrom, and H. F. MacMillan, "Minority-carrier lifetime and photon recycling in N-GaAs," J. Vac. Sci. Technol. A **10**, 990 (1992).
[7]S. Johnston, K. Zaunbrecher, R. Ahrenkiel, D. Kuciauskas, D. Albin, and W. Metzger, "Simultaneous measurement of minority-carrier lifetime in single-crystal CdTe using three transient decay techniques," *J. Photovoltaics* **4**, 1295 (2014).
[8]R. K. Ahrenkiel and S. W. Johnston, "An optical technique for measuring surface recombination velocity," Sol. Energy Mater. Sol. Cells **93**, 645–649 (2009).